AGU PUBLICATIONS

JGR

Journal of Geophysical Research: Oceans

RESEARCH ARTICLE

10.1002/2014JC010590

Strengthening Kuroshio observed at its origin during November 2010 to October 2012

Zhaohui Chen[1,2], Lixin Wu[1,2], Bo Qiu[3], Lei Li[1], Dunxin Hu[4], Chengyan Liu[5], Fan Jia[4], and Xi Liang[6]

[1]Physical Oceanography Laboratory, Ocean University of China, Qingdao, China, [2]Qingdao Collaborative Innovation Center of Marine Science and Technology, Ocean University of China, Qingdao, China, [3]Department of Oceanography, University of Hawaii at Manoa, Honolulu, Hawaii, [4]Key Laboratory of Ocean Circulation and Waves, Institute of Oceanology, Chinese Academy of Sciences, Qingdao, China, [5]Polar Climate System and Global Change Laboratory, Nanjing University of Information Science and Technology, Nanjing, China, [6]Polar Environmental Research and Forecasting Division, National Marine Environmental Forecasting Center, Beijing, China

Key Points:
- The Kuroshio at its origin is observed to increase
- It is associated with the dipole-like SSH trend east of Luzon
- The wind forcing is important for the subthermocline water property changes

Correspondence to:
Z. Chen,
chenzhaohui@ouc.edu.cn

Citation:
Chen, Z., L. Wu, B. Qiu, L. Li, D. Hu, C. Liu, F. Jia, and X. Liang (2015), Strengthening Kuroshio observed at its origin during November 2010 to October 2012, *J. Geophys. Res. Oceans*, *120*, doi:10.1002/2014JC010590.

Received 18 NOV 2014
Accepted 27 FEB 2015
Accepted article online 13 MAR 2015

Abstract Direct measurements of Kuroshio at its origin (18°N, east of the Luzon Island) are conducted from November 2010 to October 2012. It is found that the depth-averaged Kuroshio between 200 and 700 m has increased over 15 cm s^{-1} during the 2 year observational period and it is accompanied by the pronounced southward shift of the North Equatorial Current (NEC) bifurcation. Further analysis indicates that the Kuroshio's strengthening is confined to the upstream segment east of the Luzon Island while the Kuroshio decreased as it passed the Luzon Strait due to a dipole-like sea surface height (SSH) trend between 15°N and 23°N. It is demonstrated that the 2 year strengthening of the Kuroshio, as well as the dipole-like SSH trend can be adequately reproduced by a 1.5 layer nonlinear reduced gravity model, suggesting an important role of upper ocean response to low-frequency wind forcing in the western Pacific. Salinity at 500 m depth is also found to increase during the concurrent 2 years. This subthermocline salinity increase is a combined outcome of vertical (basin-scale isopycnal surface movement) and horizontal advections (i.e., strengthened Kuroshio) due to changes in the large-scale wind-driven ocean circulation.

1. Introduction

As a poleward western boundary current in the North Pacific, the Kuroshio originates from east of Luzon and flows continuously along the coast of Taiwan and the continental slope of the East China Sea until it separates from the coast of Japan [*Nitani*, 1972].The Kuroshio transports a large amount of mass, heat, and salt from low-latitude to mid-latitude/high-latitude regions, regulating the mass/heat exchange along its path and local/global climate, so the integrated monitoring of Kuroshio is in urgent need [*Send et al*., 2009]. Until now there have been some mooring observations of the upstream Kuroshio in the east of Taiwan [e.g., *Tang et al*., 2000; *Lee et al*., 2001; *Johns et al*., 2001; *Zhang et al*., 2001], yet long-term direct measurements at its origin are relatively sparse and they are still being implemented at their initial stage [*Hu et al*., 2013; *Lien et al*., 2014; *Gordon et al*., 2014].

There are few mooring studies that have focused on the Kuroshio at its origin. A recent work by *Lien et al*. [2014] analyzed an array of six moorings that were deployed at the entrance to Luzon Strait during June 2012 to June 2013, with their focus on the modulation of Kuroshio transport by mesoscale eddies. The time span of these moorings, however, was no more than 1 year. Likewise, the study of *Gordon et al*. [2014] deployed an array of moorings to observe the nascent Kuroshio in the Lamon Bay from May 2011 to May 2012, with the time span again being less than 1 year. So far, there have been zero descriptions of Kuroshio at its origin using in site mooring observations that lasted more than 1 year. It is thus urgent and beneficial to prolong the mooring observations east of the Luzon Island in order to enrich our understandings of the Kuroshio at longer timescales.

Recently two subsurface moorings were successively deployed at 18°N just off the Luzon Island in November 2010 and July 2011, respectively. Deployment of these subsurface moorings aims to maintain the long-term direct observations of the Kuroshio at its origin and is an important part of the field experiment of the Northwestern Pacific Ocean Circulation and Climate Experiment (NPOCE). Analyzing the data of the first subsurface mooring that spanned almost 8 months from November 2010 to July 2011, *Hu et al*. [2013] identified

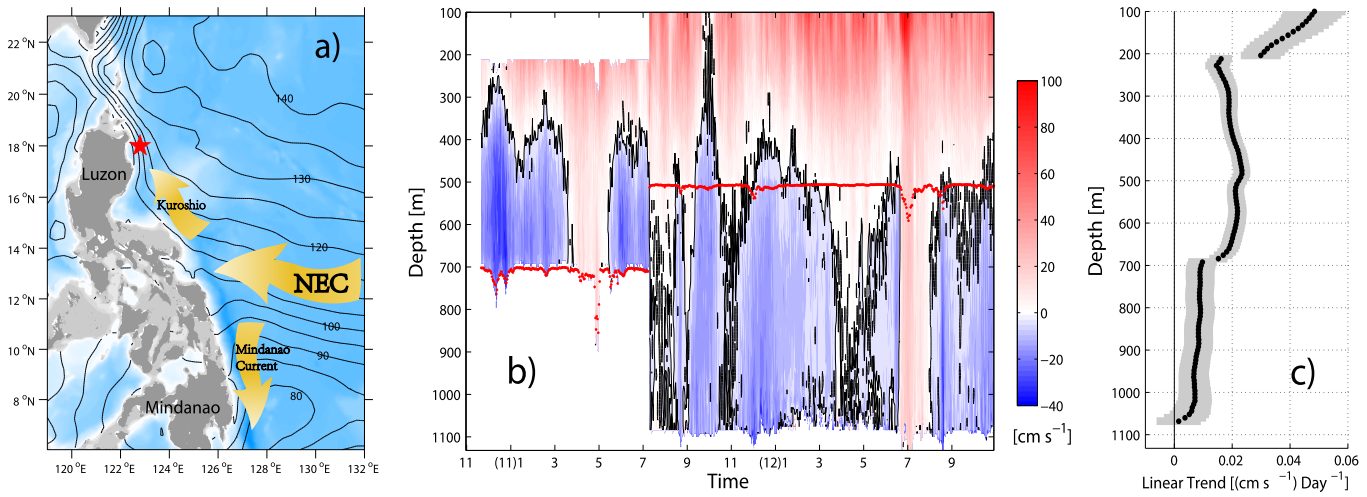

Figure 1. (a) Location of the 18°N subsurface mooring (red star). Color map in blue shows the topography east of Philippines and Luzon Strait with contours are mean sea surface height (cm) during 1992–2012 from AVISO. (b) Daily-averaged meridional velocity profiles measured by the ADCPs from November 2010 to October 2012. The black contours indicate zero line of the velocity and the red dots indicate the parking depths of subsurface moorings. (c) Linear trend of the daily-averaged meridional velocity for each level. Gray shading indicates the 95% confidence level of the trend.

some new features of the Luzon Undercurrent (LUC). They argued that significant intraseasonal variability (ISV) of about 70–80 days dominates the observed Kuroshio/LUC. Further analysis and model simulation indicate that the ISV of the LUC is dominated by eddies with diameters of about 200–300 km and extending from sea surface to an intermediate layer east of the Luzon Island [*Wang et al*., 2014].

With the subsequent second set of mooring recovered in October 2012, the direct measurement time span extended to almost 2 years (711 days). This combined mooring data set enables us to focus on not only its intraseasonal variability, but also the low-frequency change of the Kuroshio. The objectives of this study are to describe the low-frequency change of the Kuroshio at its origin during the 2 year period and to discuss the cause of this variability. The paper is organized as follows: section 2 gives a brief description of the data used in this study, followed by the results in section 3. The summary and discussion are presented in section 4.

2. Data

2.1. Mooring Data

Two subsurface moorings were successively deployed between November 2010 and October 2012. The first mooring (18.02°N, 122.63°E) that started on 20 November 2010 and ended on 10 July 2011 was deployed at about 700 m depth and was equipped by a upward-looking acoustic Doppler current profiler (75 kHz ADCP). For more detailed descriptions of the mooring, the readers are referred to *Hu et al*. [2013]. The subsequent mooring (17.96°N, 122.93°E) was deployed on 11 July 2011 after data acquisition and was finally recovered on 30 October 2012. It is worth noting that the second mooring was equipped with both upward-looking and downward-looking ADCPs with its depth at about 500 m. We also have one conductivity/temperature (CT) sensor attached to the main float to monitor the change of the temperature and salinity.

The two moorings are not far from each other and they will be regarded in this study to be deployed approximately at the same position (Figure 1a), forming a set of 2 year current data. The ADCP data are measured every 30 min and the daily-averaged time series is used in the following analyses after the removal of high-frequency tidal current signals.

2.2. Satellite Data

The delayed-time, merged, global ocean gridded absolute surface dynamic topography as well as the absolute geostrophic velocities produced by the Data Unification and Altimeter Combination System (DUACS)

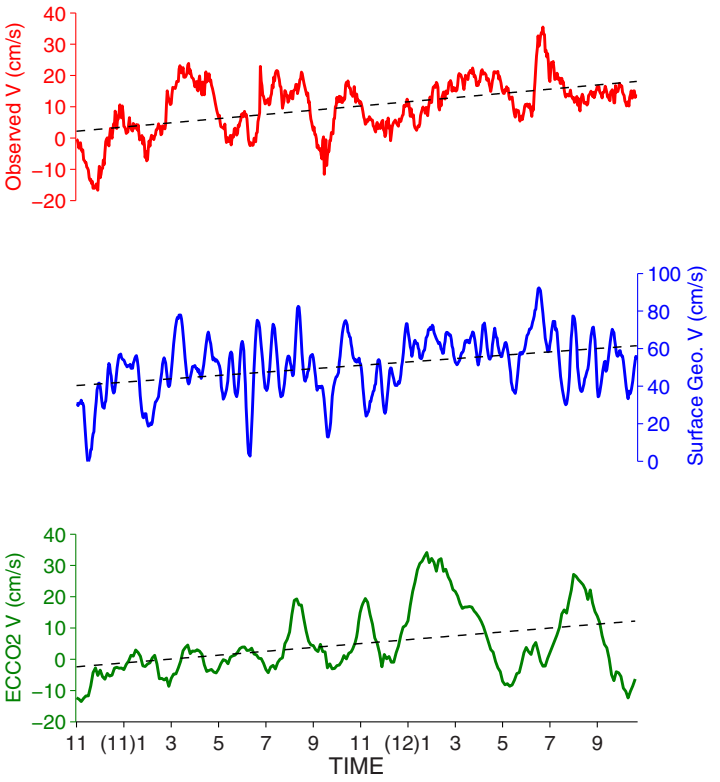

Figure 2. Time series of depth-averaged meridional velocity between 200 and 700 m from ADCPs (red), meridional component of absolute geostrophic velocities from AVISO (blue), and 200–700 m averaged meridional velocity from ECCO2 (green) at/nearest to mooring site. The dashed lines are the linear trend of each time series.

and distributed by Archiving, Validation, and Interpretation of Satellite Data in Oceanography (AVISO) are used in this study. Here, we adopt the daily-version of these data sets that overlap the mooring period.

2.3. ECCO2 Data and MOAA-GPV Data

In addition to the satellite data, we employ a recently developed Estimating the Circulation and Climate of the Ocean Phase II (ECCO2) product, which aims to produce increasingly accurate syntheses of all available global-scale ocean and sea-ice data to resolve ocean eddies and other narrow currents [*Menemenlis et al*., 2008]. The ECCO2 product provides 3 day average with a high spatial resolution (0.25° by 0.25°) to adequately diagnose the circulation variability in the western boundary current system.

We also use monthly temperature and salinity data set compiled by *Hosoda et al*. [2008] that combines quality-controlled Argo-profiling data and other available moored/ship-board observations. This data set, known as the monthly objective analysis using the Argo data (MOAA) grid point value (GPV), is available from 2001 with a spatial resolution of 1°in the upper 2000 m.

3. Results

3.1. Strengthened Kuroshio During November 2010 to October 2012

Apart from the different mooring depth, the configuration of ADCPs in the two deployments differs from each other. The first-period ADCP measures the currents in 60 bins with a bin size of 8 m, while the second-period upward-looking and downward-looking ADCPs are of 74 bins with an 8 m bin size. The sampling depth, therefore, is not uniform, with the first one ranges from 200 to 700 m and the second one from the sea surface to almost 1100 m.

In the east of the Luzon Island, the main axis of Kuroshio is basically along the north-south coastline. So the northward component of the ADCP-derived data is used to investigate the Kuroshio variability at the mooring site. It is demonstrated in Figure 1b that the northward Kuroshio exists above 400 m throughout the 2 year observational period with its maximum velocity exceeding 100 cm s^{-1}. The LUC is observed mainly below 500 m and its maximum velocity can reach 30–40 cm s^{-1}.

Superimposed on the intraseasonal variability of Kuroshio and LUC that have been reported in recent studies [*Hu et al*., 2013; *Wang et al*., 2014], the meridional velocity profile in Figure 1b reveals a downward shifting of the zero velocity contour, implying an enhanced northward anomalous flow within the whole observed layer at the mooring site. To verify the nature of this full-depth change, we plot the magnitude of 2 year trend for each level and find that both the upper layer Kuroshio and the lower layer LUC share the same trend, i.e., strengthening northward during November 2010 to October 2012 (Figure 1c).

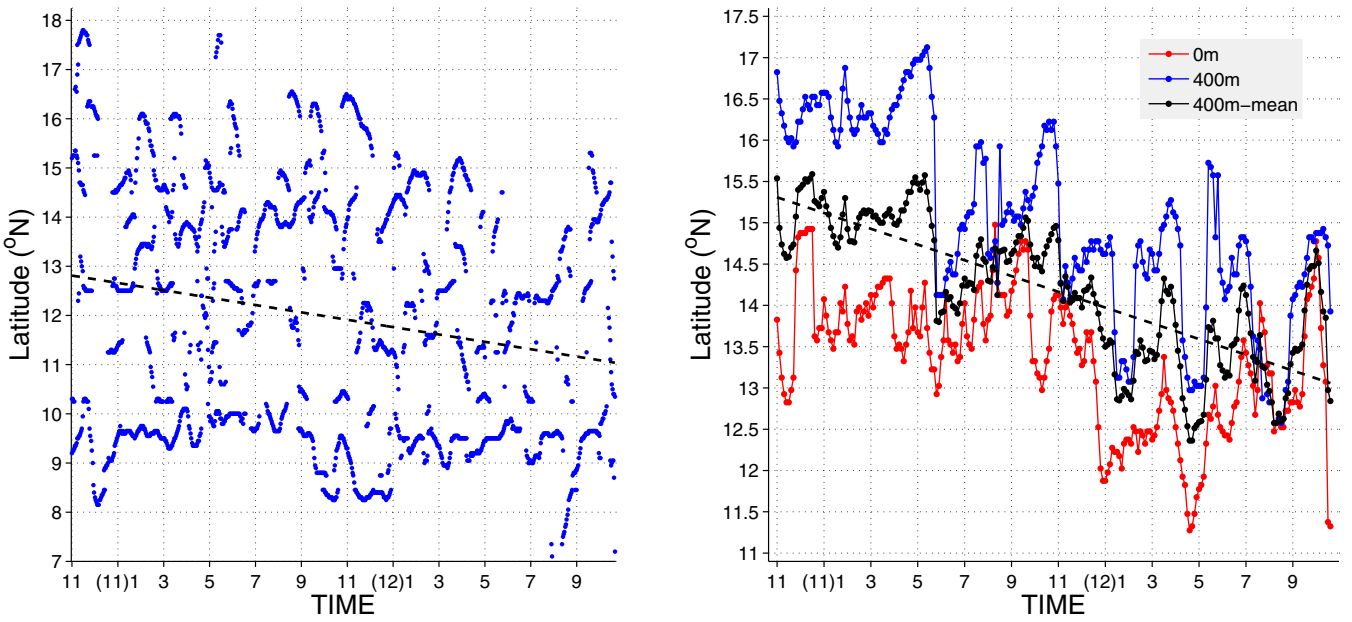

Figure 3. (left) Scattered bifurcation points estimated from AVISO daily geostrophic velocities averaged within 2° band off the Philippine coast. The dashed line indicates linear fitting of these points. (Right) Time series of the NEC bifurcation latitude at surface (red), 400 m depth (blue), and upper 400 m mean (black) derived from ECCO2 products. The dashed line in black denotes the linear trend of the 400 m mean bifurcation latitude.

To better illustrate the 2 year trend of the Kuroshio, a depth-averaged meridional velocity measured by ADCP is derived between 200 and 700 m. In addition, the meridional component of absolute geostrophic velocities from AVISO and 200–700 m averaged flow from ECCO2 at the grid point nearest to the mooring site during the overlapped period are plotted. It is shown in Figure 2a that the depth-averaged meridional velocity exhibits a significant trend (almost 16 cm s^{-1} per the 2 year period), indicating the Kuroshio has strengthened during the 2 year observations, although it has decreased a little bit over the last 5 months. This observed feature is further validated by the altimetry-derived surface geostrophic flow and the model assimilated depth-averaged flow. The surface geostrophic meridional velocity presents a significant trend with a 20 cm s^{-1} increase during the 2 year period and the depth-averaged meridional velocity between 200 and 700 m derived from ECCO2 exhibits a 14 cm s^{-1} increase (Figures 2b and 2c).

3.2. Associated Ocean Circulation Change

The analysis above demonstrated that the observed Kuroshio has undergone a 2 year increase at its origin. This implies that the NEC bifurcation latitude, which is an important indicator of the Kuroshio/Mindanao Current (MC) partitioning at their origins, should have shifted southward accordingly [e.g., *Qiu and Lukas*, 1996; *Kim et al*., 2004; *Qiu and Chen*, 2010a]. To verify whether the strengthened Kuroshio is accompanied by the southward migration of the NEC bifurcation, we plot in Figure 3 the NEC bifurcation time series derived from the AVISO and ECCO2 data during the observational period.

Our definition for the NEC bifurcation follows the method of previous studies and it is where the meridional flow within the 2° band off the Philippine coast is zero [*Chen and Wu*, 2012]. The result is not sensitive to the averaging band width particularly when we focus on the NEC's low-frequency migration. It should be emphasized that due to the high spatial/temporal variability of the AVISO daily geostrophic velocities, one cannot obtain the bifurcation latitude straightforward since there are several zero-velocity points along the Philippine coast. Under such circumstances, we plot each point where the meridional velocity varies from negative to positive toward the north, and the 2 year migration of the NEC bifurcation is represented by the linear fitting of all possible scattered bifurcation points.

It is shown in Figure 3 that the NEC bifurcation at the surface shifted southward for over 1.8° and that the upper 400 m mean bifurcation shifted southward for 2.2° from the ECCO2 product during the observational period, which is consistent with the increased meridional component of the Kuroshio velocity as shown in Figures 2b and 2c. It should be noted in Figure 3a that the scattered points at their southernmost positions remain

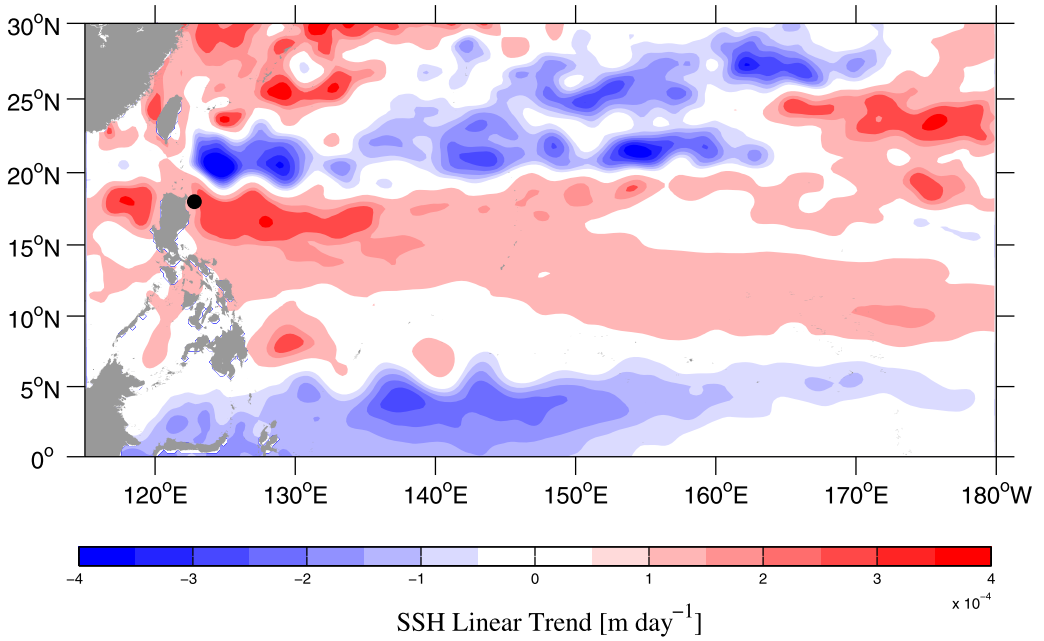

Figure 4. Linear trend of AVISO daily SSH from 20 November 2010 to 30 October 2012. The black dot indicates the position of the moorings.

unchanged, while their northernmost positions exhibit significant southward migration. This has an implication that enhanced positive SSH may be only confined to the north of the mean bifurcation latitude according to the correlation map between bifurcation and SSH [*Qiu and Chen*, 2010a], while it is not significant in the south during the 2 year period.

To verify the associated SSH change in the western Pacific, we further examine its linear trend during the 2 year period, because previous studies have indicated changes in both the Kuroshio and the NEC bifurcation are manifestations of basin-scale circulation that can be deduced from the SSH maps [*Wang and Hu*, 2006; *Qiu and Chen*, 2010a]. To relate the observed trend of the Kuroshio to the broad-scale circulation changes, we plot the linear trend of SSH in Figure 4. It is shown that, during the 2 year observational period, the SSH trend has a spatially nonuniform structure: it rises in the east of the Philippines and falls on both sides of this rising band. East of the Luzon Island/Strait, a remarkable dipole-like SSH trend pattern exists in the region of15°–23°N, 123°–135°E, with a positive SSH trend core in the east of the Luzon Island and a negative SSH trend core in the east of the Luzon Strait. Along the Kuroshio paths from 15°N to 23°N, the dipole-like pattern increases/decreases the zonal pressure gradient, leading to strengthened/weakened Kuroshio according to geostrophy. Therefore, the strengthened Kuroshio is only confined to its upstream path south of about 19°N.

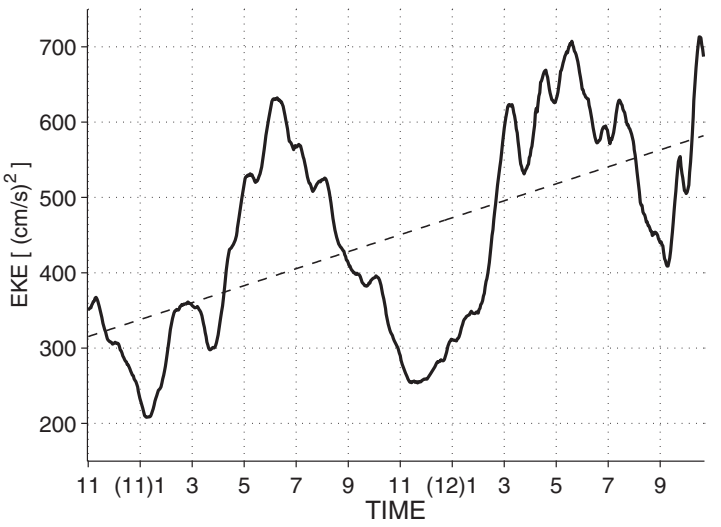

Figure 5. Time series of eddy kinetic energy (EKE) averaged in [18°–23°N,123°–140°E] derived from AVISO daily geostrophic velocities following *Qiu* [1999]. The dashed line is the linear trend.

In the same way, the strengthened Subtropical Countercurrent (STCC) can be inferred from the dipole-like SSH trend.

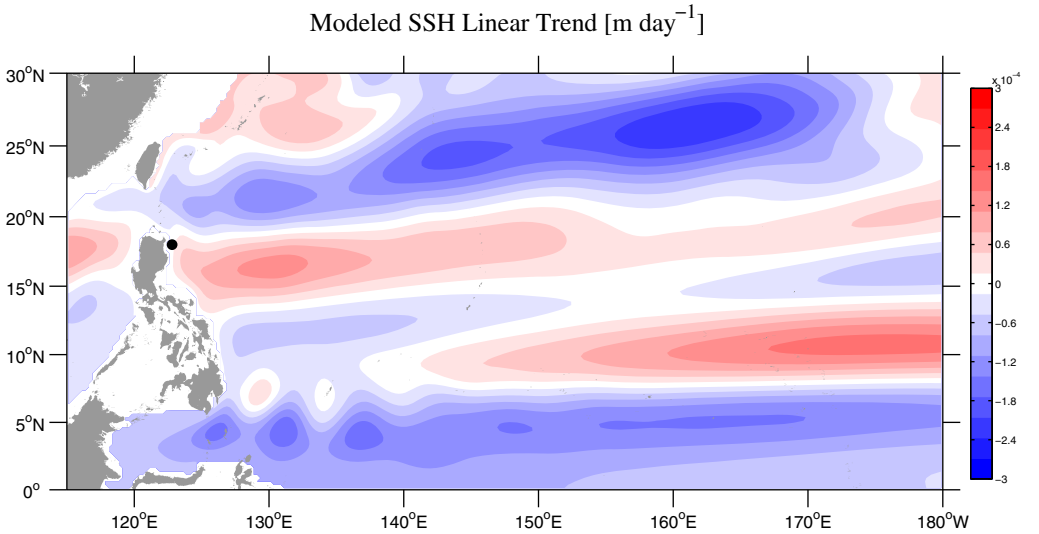

Figure 6. Same as Figure 4, but for the linear trend of simulated SSH by a 1.5 layer nonlinear reduced gravity model.

The STCC is an eddy abundant region and the strengthened STCC can enhance the vertical shear with the underlying NEC [*Qiu*, 1999; *Qiu and Chen*, 2010b], so it is not surprising that the eddy kinetic energy (EKE) in this region presented an increasing trend (Figure 5).

3.3. Model the Pattern of SSH Trend

To understand the cause of strengthening Kuroshio during November 2010 to October 2012, we use a simple model in this section to reproduce the above-mentioned SSH trend, in particular, the dipole-like SSH pattern east of the Luzon Island/Strait. Here we adopt a 1.5 layer nonlinear reduced gravity model that has been proven to be dynamically relevant in the studies of tropical upper ocean circulation in the Pacific, Atlantic and Indian Oceans [e.g., *Qiu and Lukas*, 1996; *Yang and Joyce*, 2006; *Chen and Wu*, 2011; *Chen et al.*, 2014].

The governing equations of the 1.5 layer nonlinear reduced gravity model are:

$$\frac{\partial u}{\partial t}+u\frac{\partial u}{\partial x}+v\frac{\partial u}{\partial y}-fv+g'\frac{\partial h}{\partial x}=A_H\nabla^2 u+\frac{\tau^x}{\rho h} \quad (1)$$

$$\frac{\partial v}{\partial t}+u\frac{\partial v}{\partial x}+v\frac{\partial v}{\partial y}+fu+g'\frac{\partial h}{\partial y}=A_H\nabla^2 v+\frac{\tau^y}{\rho h} \quad (2)$$

$$\frac{\partial h}{\partial t}+\frac{\partial hu}{\partial x}+\frac{\partial hv}{\partial y}=0 \quad (3)$$

where u and v are the zonal and meridional velocity, h the upper layer thickness, f the Coriolis parameter, g' the reduced gravity acceleration, A_H the coefficient of horizontal eddy viscosity (2000 m^2 s^{-1}), ρ the reference water density, and τ^x and τ^y the zonal and meridional surface wind stresses, respectively. The initial upper layer thickness is $H = 350$ m, corresponding to the mean depth of 26.7 σ_θ in the North Pacific derived from the World Ocean Atlas 2009 (WOA09) (see Figure 2 in *Chen and Wu*, [2011]). Here g' in the model is chosen to be 0.033 m s^{-2}. The model domain covers the subtropical and tropical North Pacific and extends from 20°S to 40°N in the meridional direction and from 100°E to 70°W in the zonal direction. The horizontal resolution of the model is 0.25° and marginal seas shallower than 200 m are treated as land. The model is forced by daily wind stresses provided by ECCO2 from January 1992 to December 2012. Outputs from the 711 days overlapping with the mooring measurements are used to calculate the linear trend of the modeled SSH.

It is demonstrated in Figure 6 that the model well reproduced the observed SSH trend pattern during the overlapping period, although its magnitude is weaker. The disparity in the magnitude of SSH trend may stem from the smoothed wind stress forcing and/or the absence of complex physical processes in this simple model. We also conducted some experiments by selecting different g' and H ensuring that the gravity

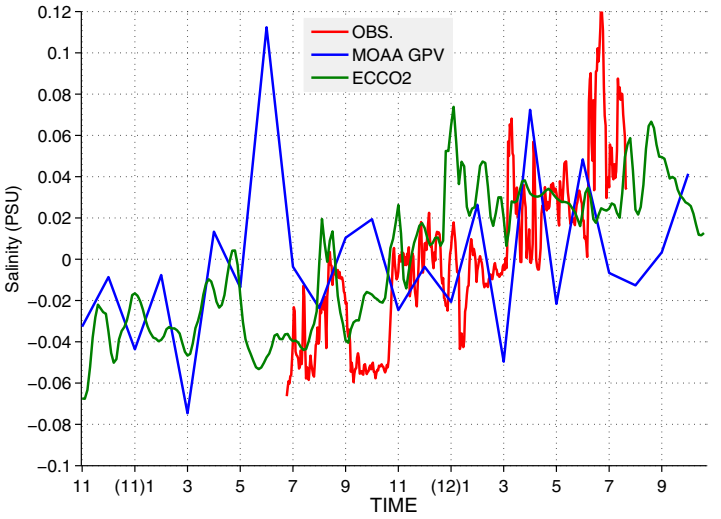

Figure 7. Time series of salinity anomaly by (red) daily CT measurement, (blue) monthly mean MOAA-GPV data, and (green) 3 day mean ECCO2 data at/nearest to mooring site.

wave speed c ranges from 2.9 to 3.6 m s^{-1}. It is found that linear trend in modeled SSH is not sensitive to the choice of c (figure not shown). In general, the model captures the main feature of the SSH trend, for instance, the dipole-like pattern east of the Luzon Island/Strait, as well as the decreasing SSH in the subtropical Northwestern Pacific and North Equatorial Countercurrent (NECC) regions. This explicitly indicates the low-frequency change in the wind stress forcing accounts for the spatial distribution of the observed SSH trend, or the observed Kuroshio trend, through the first-mode baroclinic adjustment processes. We also apply a linear, reduced gravity, long Rossby wave model and a 2.5 layer nonlinear reduced gravity model for our tests and they exhibit almost the same modeled SSH trends (not shown). This is indicative of minor effects of nonlinearity and high-order baroclinic processes.

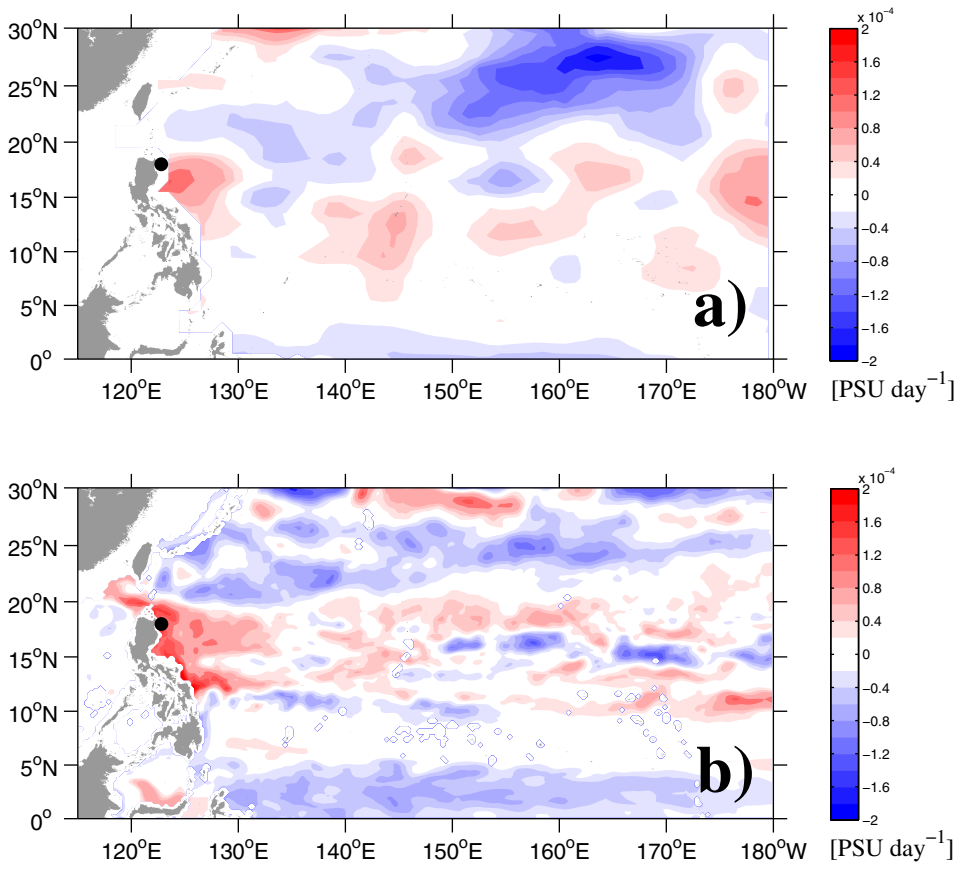

Figure 8. Linear trend of salinity derived from (a) MOAA-GPV and (b) ECCO2 at 500 m during the 2 year period.

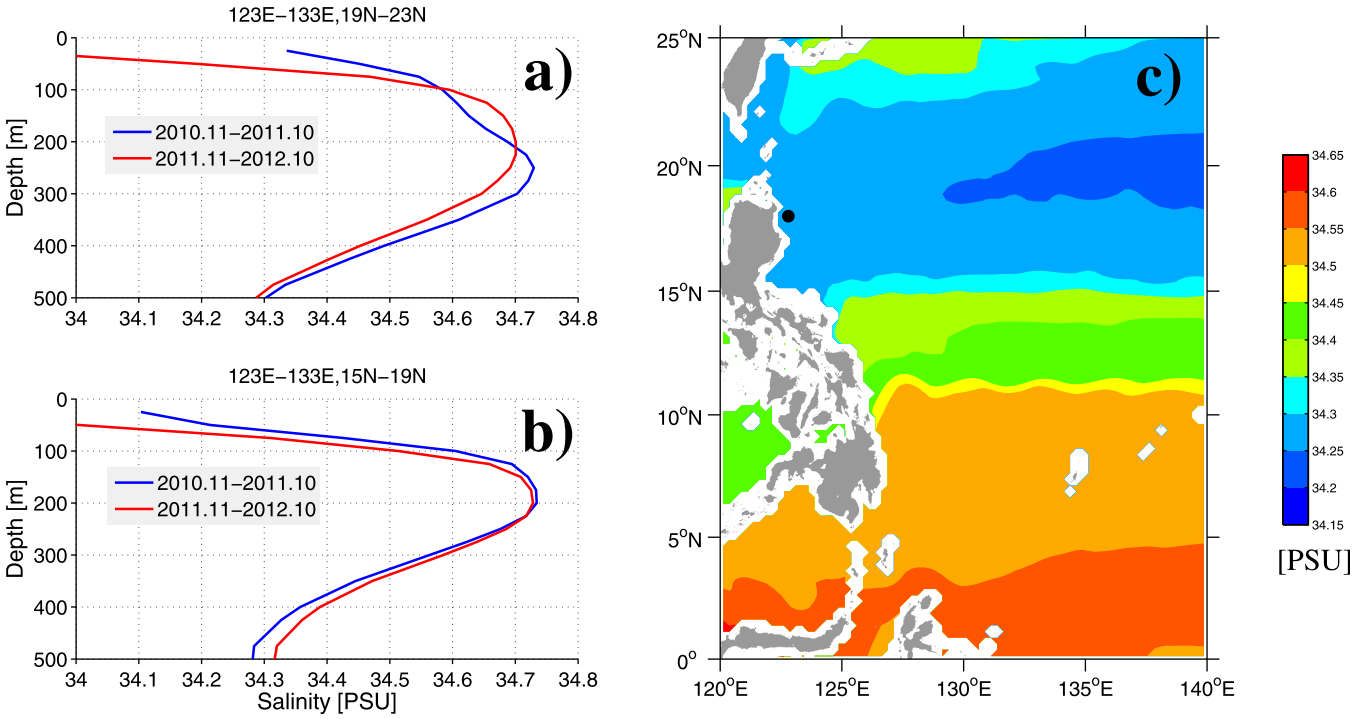

Figure 9. Yearly mean vertical salinity profiles averaged in (a) [123–133°E, 19°–23°N] and (b) [123°–133°E, 15°–19°N] from ECCO2. (c) Climatological mean of 500 m salinity distribution from ECCO2.

3.4. Observed Salinity Trend

In addition to the direct measurement of current velocity, we examine the 500 m depth salinity variability derived from the CT sensor that is mounted on the main float during the second mooring period. It is shown in Figure 7 that the salinity underwent a significant increasing trend during the second mooring period from 11 July 2011 to 1 August 2012. We extend the time series of salinity from ECCO2 and MOAA-GPV and find that this increasing trend is consistent and significant during the overlapping period (Figure 7).

To address the cause of the increasing salinity trend at the mooring site, it is beneficial to first check the broad-scale pattern of salinity change at 500 m depth. Figure 8 shows the spatial pattern of the linear trend of salinity at 500 m in ECCO2 and MOAA-GPV, respectively. Interestingly, the salinity signal also exhibits a distinct broad-scale change in the Northwestern Pacific, with more saline water in the east of the Philippines and less on both sides. This salinity trend pattern is quite similar to that of the SSH, particularly the dipole-like pattern, indicating a close relationship between the broad-scale change in salinity and SSH.

Here we highlight that the SSH-related salinity trend is associated with vertical advection caused by the movement of isopycnal surfaces. As we have shown in Figure 4, an order of 10^{-4} m day^{-1} in SSH corresponds to 25 m rise/fall in isopycnal layers over the 2 year period, and this will lead to changes in salinity at fixed depths below the mixed layer. An examination of the vertical salinity profiles from ECCO2 product indicates that the salinity profile becomes less (more) saline in the northern (southern) dipole region in the second year below 300 m (Figures 9a and 9b). With the mooring site located inside the southern dipole, this result suggests that the vertical displacement of isopycnal layers is important, at least partially, for the observed salinity increase at 500 m at the mooring site.

Aside from the SSH-related salinity trend, the increasing trend of salinity is more prominent along the Philippine coast (Figure 8). Here, we examine the potential temperature-salinity (T-S) relations using the MOAA GPV data to quantify the role of horizontal advection relating to the enhanced Kuroshio that advects northward the saltier water from NEC (Figure 9c). It is shown in Figure 10a that in the region away from the Philippine coast, both of the temperature and salinity at 500 m depth have increased over the 2 year period, despite that the increase of salinity is not as prominent as temperature. Moreover, the potential density of

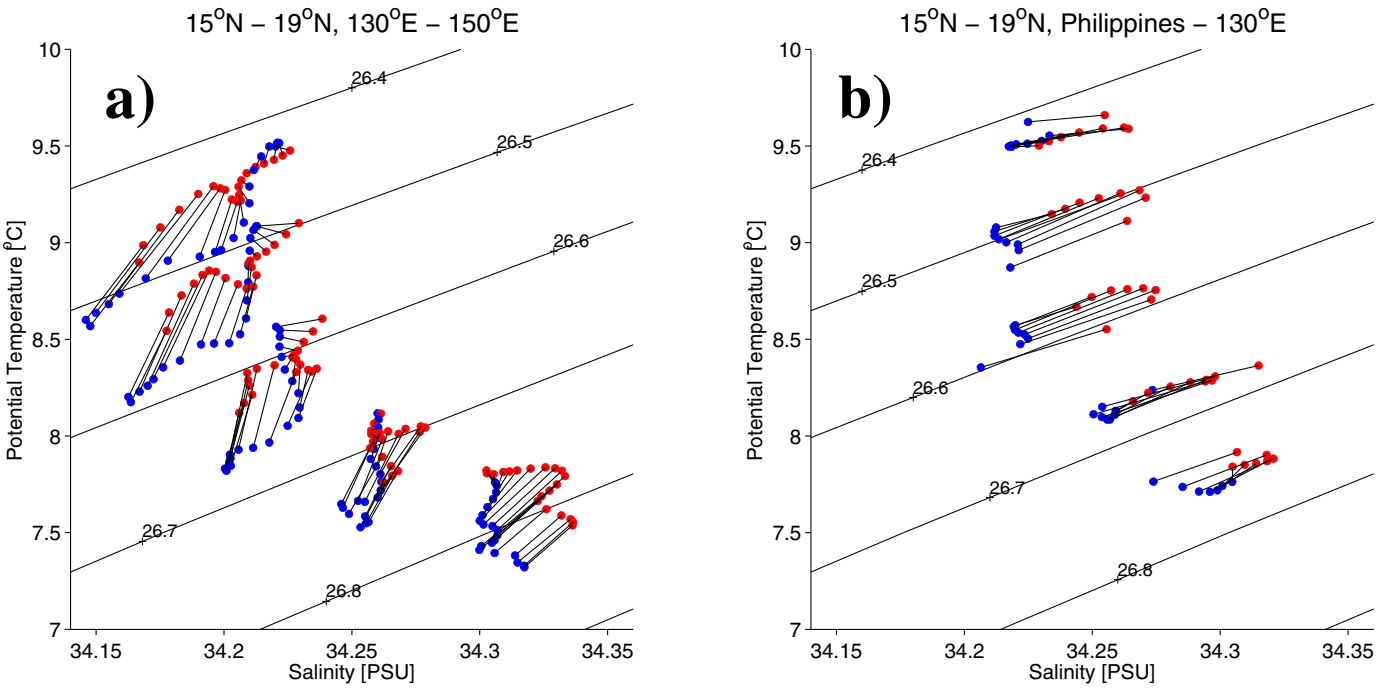

Figure 10. T-S plot at 500m in the box (a) 15–19°N, 130–150°E, and (b) 15–19°N, Philippine coast to130°E. The T-S values are derived from MOAA-GPV data by averaging the data in November 2010 to October 2011 (blue) and November 2011 to October 2012 (red).

water masses at this depth decreased consistently, in agreement with the downward shifting of isopycnal surfaces due to increasing SSH. Near the Philippine coast, however, the T-S relations still exhibit an increase pattern but the potential density remain unchanged (Figure 10b). This implies that the horizontal advection dominates the increasing of salinity due to enhanced Kuroshio east of the Luzon Island. Thus, the observed increasing salinity is likely a combined outcome of both vertical and horizontal advections due to the large-scale wind-forced circulation change.

4. Summary and Discussions

In this study, we analyzed the 2 year direct measurements of the Kuroshio approximately at 18°N, east of the Luzon Island. It is found that the Kuroshio exhibits an increasing trend at all depths during the observational period from 20 November 2010 to 30 October 2012. The depth-averaged Kuroshio between 200 and 700 m has increased over 15 cm s^{-1} during the 2 year observation and this is associated with a pronounced southward shift of the North Equatorial Current (NEC) bifurcation.

Further analysis indicates that the strengthened Kuroshio is only confined to its origin, i.e., in its upstream region east of the Luzon Island, while it decreased as it passed the Luzon Strait. This is due to a dipole-like sea surface height (SSH) trend between 15°N and 23°N, which enhances the Kuroshio south of 19°N and weakens it north of 19°N according to geostrophy. In addition, the SSH trend pattern favors an increasing eastward flow along ~19°N and intensifies the vertical shear between STCC and the underlying NEC, leading to stronger eddy activities along this band.

We adopt a 1.5 layer nonlinear reduced gravity model, forced by the ECCO2 daily wind stress, to simulate the SSH trend during the 2 years of our mooring measurements. It is shown that the model can adequately reproduce the strengthened Kuroshio and the SSH pattern, in particular, the dipole-like SSH trend. This suggests an important role of the upper ocean response to low-frequency wind forcing within the framework of baroclinic Rossby wave dynamics in the tropical Pacific.

It is further shown that the observed salinity also exhibits an increasing trend by the CT measurement that is mounted on the main float at 500 m. The increasing salinity at this depth is found to be

associated with both vertical advection (relating to the basin-scale isopycnal surfaces movement) and horizontal advection (relating to the strengthened Kuroshio) that are due to changes in the large-scale ocean circulation. Considering the resemblance between the 500 m salinity and SSH pattern, it is important to stress that the surface wind forcing is not only important for the upper ocean circulation variability, but also for the subthermocline water property changes. This latter point has not been emphasized in previous studies.

It should be noted that the 2 year mooring period corresponds to the 2011/2012 La Niña period and the result that the Kuroshio transport near its origin strengthens during an La Niña event is consistent with the previous modeling studies [*Qiu and Lukas*, 1996; *Kim et al*., 2004]. However, a further analysis using the 20 year AVISO data does not support the close interannual relationship between the Kuroshio and climate indices (e.g., El Niño and Southern Oscillation, ENSO; Pacific Decadal Oscillation, PDO). The interannual correlation between the monthly surface geostrophic velocity at the mooring site and Nino3.4 index (PDO index) is 0.05 (−0.09), much less than that between the NEC bifurcation latitude and the climate indexes (0.65 for Nino3.4 and 0.74 for PDO). This implies that the bifurcation latitude is not indicative of changes in the upstream Kuroshio east of the Luzon Island. The concurrent Kuroshio strengthening and southward shift of bifurcation may be associated with recent high correlation between ENSO and the interannual variability in the low-latitude western North Pacific as PDO shifts to its cold phase, as suggested by *Wu* [2013]. Given the availability of the 2 year mooring data, it is difficult at this point to ascertain whether the observed Kuroshio change is more related to the PDO-related wind forcing, as compared to the La Niña-related wind forcing. Thus, the interannual relationship between the Kuroshio and the climate indices needs further investigations.

Another point we should emphasize is the insufficient simulation of the SSH trend magnitude using the model although it well reproduced the spatial pattern of this trend. In addition to the issue of smoothed wind forcing from the ECCO2 product, an important potential contributor may come from the oceanic eddy forcing. The regional sea level trend in the Pacific Ocean has been considered to be induced by low-frequency changes in surface wind, while this trend can also be generated by eddy momentum flux forcing due to time-varying instability of the background circulation. We have shown that the eddy activities in the STCC region exhibit an increasing trend during the 2 year observational period, so it is speculated that the enhanced eddy activities may contribute to the magnitude of the SSH trend through the eddy forcing on mean flow [*Haidvogel and Rhines*, 1983; *Qiu et al*., 2015].

Finally, we note that the variability of both the upper layer Kuroshio and the lower-layer LUC share the same features from intraseasonal to interannual time scales. As such, it is possible to deduce the LUC's changes from the time-varying SSH maps constructed from the satellite altimetry measurements.

Acknowledgments

We express our sincere gratitude to the crew of R/VScience 1, including all scientists and technicians on board for deployment and retrieval of the two subsurface moorings. The altimeter products used in this analysis were produced by Ssalto/Duacs and distributed by Aviso, with support from CNES (http://www.aviso.oceanobs.com/duacs/).The ECCO2 product was accessed from ftp://ecco2.jpl.nasa.gov/ and the MOAA-GPV product fromftp://ftp2.jamstec.go.jp/pub/argo/MOAA_GPV/Glb_PRS/OI/. This research is supported by the National Science Foundation of China (41306001, 41130859, 41221063, U1406401), the National Basic Research Program of China (2013CB956201), the Global change project (GASI-03-01-01-05), and the provincial/ministerial-level projects (BS2013HZ010, XDA11010101).

References

Chen, Z., and L. Wu (2011), Dynamics of the seasonal variation of the North equatorial current bifurcation, *J. Geophys. Res.*, *116*, C02018, doi:10.1029/2010JC006664.

Chen, Z., and L. Wu (2012), Long-term change of the Pacific North equatorial current bifurcation in SODA, *J. Geophys. Res.*, *117*, C06016, doi:10.1029/2011JC007814.

Chen, Z., L. Wu, B. Qiu, S. Sun, and F. Jia (2014), Seasonal variation of the south equatorial current bifurcation off Madagascar, *J. Phys. Oceanogr.*, *44*, 618–631.

Gordon, A. L., P. Flament, C. Villanoy, and L. Centurioni (2014), The nascent Kuroshio of Lamon Bay, *J. Geophys. Res. Oceans*, *119*, 4251–4263, doi:10.1002/2014JC009882.

Haidvogel, D., and P. Rhines (1983), Waves and circulation driven by oscillatory winds in an idealized ocean basin, *Geophys. Astrophys. Fluid Dyn.*, *25*, 1–63.

Hosoda, S., T. Ohira, and T. Nakamura (2008), A monthly mean dataset of global oceanic temperature and salinity derived from Argo float observations, *JAMSTEC Rep. Res. Dev.*, *8*, 47–59.

Hu, D., S. Hu, L. Wu, L. Li, L. Zhang, X. Diao, Z. Chen, Y. Li, F. Wang, and D. Yuan (2013), Direct measurements of the Luzon undercurrent, *J. Phys. Oceanogr.*, *43*(7), 1417–1425.

Johns, W., T. N. Lee, D. Zhang, R. Zantopp, C.-T. Liu, and Y. Yang (2001), The Kuroshio east of Taiwan: Moored transport observations from the WOCE PCM-1 array, *J. Phys. Oceanogr.*, *31*, 1031–1053.

Kim, Y. Y., T. Qu, T. Jensen, T. Miyama, H. Mitsudera, H.-W. Kang, and A. Ishida (2004), Seasonal and interannual variations of the North equatorial current bifurcation in a high-resolution OGCM, *J. Geophys. Res.*, *109*, C03040, doi:10.1029/2003JC002013.

Lee, T. N., W. E. Johns, C.-T. Liu, D. Zhang, R. Zantopp, and Y. Yang (2001), Mean transport and seasonal cycle of the Kuroshio east of Taiwan with comparison to the Florida Current, *J. Geophys. Res.*, *106*(C10), 22,143–22,158.

Lien, R.-C., B. Ma, Y.-H. Cheng, C.-R. Ho, B. Qiu, C. M. Lee, and M.-H. Chang (2014), Modulation of Kuroshio transport by mesoscale eddies at the Luzon strait entrance, *J. Geophys. Res. Oceans*, *119*, 2129–2142, doi:10.1002/2013JC009548.

Menemenlis, D., J. M. Campin, P. Heimbach, C. Hill, T. Lee, A. Nguyen, M. Schodlok, and H. Zhang (2008), ECCO2: High resolution global ocean and sea ice data synthesis, *Mercator Ocean Q. Newsl.*, *31*, 13–21.

Nitani, H. (1972), *Beginning of the Kuroshio, Kuroshio: Its Physical Aspects*, edited by H. Stommel and K. Yoshida, pp. 129–163, Univ. of Tokyo Press, Tokyo.

Qiu, B. (1999), Seasonal eddy field modulation of the North Pacific subtropical countercurrent: TOPEX/POSEIDON observations and theory, *J. Phys. Oceanogr.*, *29*, 2471–2468.

Qiu, B., and R. Lukas (1996), Seasonal and interannual variability of the North equatorial current, the Mindanao current and the Kuroshio along the Pacific western boundary, *J. Geophys. Res.*, *101*(C5), 12,315–12,330.

Qiu, B. and S. Chen (2010a), Interannual-to-decadal variability in the bifurcation of the North equatorial current off the Philippines, *J. Phys. Oceanogr.*, *40*, 2525–2538.

Qiu, B., and S. Chen (2010b), Interannual variability of the North Pacific subtropical countercurrent and its associated mesoscale eddy field, *J. Phys. Oceanogr.*, *40*, 213–225.

Qiu, B., S. Chen, L. Wu, and S., Kida (2015), Wind- versus eddy-forced regional sea level trends and variability in the North Pacific Ocean. *J. Clim.*, *28*, 1561–1577.

Send, U., et al. (2009), A global boundary current circulation observing network, "Community White Paper Title", in *Proceedings of the "OceanObs'09: Sustained Ocean Observations and Information for Society" Conference (Vol. 2), Venice, Italy*, edited by J. Hall, D. E. Harrison, and D. Stammer, *ESA Publ. WPP-306, 2010*, 21–25 Sept.

Send, U., et al. (2010), "A global boundary current circulation observing network" in *Proceedings of OceanObs'09: Sustained Ocean Observations and Information for Society*, vol. 2, edited by J. Hall, D. E. Harrison, and D. Stammer, ESA Publication WPP-306, 21–25 September 2009, Venice, Italy, doi:10.5270/OceanObs09.cwp.78.

Tang, T., J. Tai, and Y. Yang (2000), The flow pattern north of Taiwan and the migration of the Kuroshio, *Cont. Shelf Res.*, *20*(4), 349–371.

Wang, Q., and D. Hu (2006), Bifurcation of the North equatorial current derived from altimetry in the Pacific Ocean, *J. Hydrodyn.*, *18*(5), 620–626, doi:10.1016/S1001-6058(06)60144-3.

Wang, Q., F. Zhai, and D. Hu (2014), Variations of Luzon undercurrent from observations and numerical model simulations, *J. Geophys. Res. Oceans*, *119*, 3792–3805, doi:10.1002/2013JC009694.

Wu, C.-R. (2013), Interannual modulation of the Pacific Decadal Oscillation (PDO) on the low-latitude western North Pacific, *Prog.Oceanogr.*, *110*, 49–58, doi:10.1016/j.pocean.2012.12.001.

Yang, J., and T. Joyce (2006), Local and equatorial forcing of seasonal variations of the North equatorial countercurrent in the Atlantic Ocean, *J. Phys. Oceanogr.*, *36*, 238–254.

Zhang, D., T. N. Lee, W. Johns, C.-T. Liu, and R. Zantopp (2001), The Kuroshio east of Taiwan: Modes of variability and relationship to interior ocean mesoscale eddies, *J. Phys. Oceanogr.*, *31*, 1054–1074.